J. Cent. South Univ. (2015) 22: 717−726
DOI: 10.1007/s11771-015-2575-x

Springer

Convective heat and mass transfer effects in three-dimensional flow of Maxwell fluid over a stretching surface with heat source

T. Hayat[1, 2], M. Bilal Ashraf[1], A. Alsaedi[2], S. A. Shehzad[1]

1. Department of Mathematics, Quaid-i-Azam University 45320, Islamabad 44000, Pakistan;
2. Nonlinear Analysis and Applied Mathematics (NAAM) Research Group, Department of Mathematics, Faculty of Science, King Abdulaziz University, P. O. Box 80257, Jeddah 21589, Saudi Arabia

Abstract: Heat and mass transfer effects in three-dimensional flow of Maxwell fluid over a stretching surface were addressed. Analysis was performed in the presence of internal heat generation/absorption. Concentration and thermal buoyancy effects were accounted. Convective boundary conditions for heat and mass transfer analysis were explored. Series solutions of the resulting problem were developed. Effects of mixed convection, internal heat generation/absorption parameter and Biot numbers on the dimensionless velocity, temperature and concentration distributions were illustrated graphically. Numerical values of local Nusselt and Sherwood numbers were obtained and analyzed for all the physical parameters. It is found that both thermal and concentration boundary layer thicknesses are decreasing functions of stretching ratio. Variations of mixed convection parameter and concentration buoyancy parameter on the velocity profiles and associated boundary layer thicknesses are enhanced. Velocity profiles and temperature increase in the case of internal heat generation while they reduce for heat absorption. Heat transfer Biot number increases the thermal boundary layer thickness and temperature. Also concentration and its associated boundary layer are enhanced with an increase in mass transfer Biot number. The local Nusselt and Sherwood numbers have quite similar behaviors for increasing values of mixed convection parameter, concentration buoyancy parameter and Deborah number.

Key words: Maxwell fluid; mixed convection; convective conditions; three-dimensional flow; internal heat generation/absorption

1 Introduction

Combined heat and mass transfer effects are very significant in the fields of chemical processing equipment, formation and dispersion of fog, distribution of temperature and moisture of agricultural fields and groves of fruit trees, damage of crops due to freezing and pollution of environment. Their combined effects are also useful in the cooling process of plastic sheets, glass materials and in drying processes of paper. The laminar boundary layer flow of fluids over a stretching surface is an important subject from theoretical as well as practical points of view because of their wide range of applications of such flows in polymer technology and industrial manufacturing process. Some examples are in the extrusion of polymer in a melt-spinning process, metals and plastics. Initially, CRANE [1] investigated the boundary layer flow by a stretching sheet. He obtained closed form solution for flow induced by a sheet moving with linear velocity. Later, the Crane's research problem was examined extensively through various aspects. However, mostly the fluids in the industrial and engineering processes are non-Newtonian in nature, which obey nonlinear constitutive equations. Rheological parameters in the constitutive equations add complexities in the resulting differential systems. Analytic solutions to such differential systems are rare, even the situation does not improve when one reports to approximate theories such as creeping flow or boundary layer theory, thus computational rheology is an active area of research amongst the investigators. The rheological fluids in general have been classified into three categories known as the differential, integral and rate types. The subclasses of differential type fluids namely the power law and second and third grade fluids are analyzed significantly in the existing attempts [2−6]. A subclass of rate type fluid known as the Maxwell model has been also studied [7−10].

Mixed convection flows, or combined free and forced convection flows, occur in many technological and industrial applications and in nature for example, in solar receivers exposed to wind currents, electronic devices cooled by fans, nuclear reactors cooled during emergency shutdown, heat exchanges placed in a low-velocity environment, flows in the ocean and in the atmosphere, and many more. MUKHOPADHYAY [11] analyzed the unsteady mixed convection flow and heat

Received date: 2014−04−09; **Accepted date:** 2014−07−04
Corresponding author: M. Bilal Ashraf; E-mail: bilalashraf_qau@yahoo.com

transfer over a stretching sheet in the presence of slip effects. A comprehensive study of two-dimensional mixed convection stagnation flow of an incompressible micropolar fluid with heat transfer characteristics towards a heated shrinking sheet was analyzed by RASHIDI et al [12]. Also, MORADI et al [13] studied the thermal process of the mixed convection−radiation of an inclined flat plate embedded in a porous medium. Recently, TURKYILMAZOGLU [14] investigated the analytical solution of mixed convection heat transfer and fluid flow of MHD viscoelastic fluid over a permeable stretching surface.

A study of utilizing heat source or sink in moving fluids has been a subject of interest of many researchers because of its possible application to geophysical sciences, astrophysical sciences, and in cosmical studies. Such flows arise either due to unsteady motion of the boundary or the boundary temperature. The study of fluctuating flow is important in the paper industry and many other technological fields. ELBASHBESHY and ALDAWODY [15] studied the unsteady boundary layer flow of an incompressible fluid over a stretching surface in the presence of heat source. Radiative flow of Jeffery fluid in a porous medium with power law heat flux and heat source is examined by HAYAT et al [16]. Recently, KANDASAMY et al [17] presented the combined effect of thermal diffusion and diffusion thermo on free convective heat and mass transfer over a porous stretching surface in the presence of thermophoresis particle deposition and heat source/sink.

In recent years, investigations on the boundary layer flow with convective surface boundary condition have gained much interest since the work of AZIZ [18]. In this work, the thermal boundary layer flow over a flat plate with convective surface boundary condition is examined. Later on, MAKINDE and AZIZ [19] also discussed the boundary layer flow of nanofluid past a stretching sheet with a convective boundary condition. SHEHZAD et al [20] also presented the analytical solution of three-dimensional flow of Jeffery fluid with convective surface boundary conditions.

The object of present attempt is to study the three-dimensional flow of Maxwell fluid in the presence of internal heat generation/absorption. Mixed convection effects along with heat and mass transfer are taken into account. We also considered convective type boundary conditions for both heat and mass transfer. To our knowledge, such attempt is not available in literatures. Homotopy analysis method [21−30] was employed to obtain the series solutions of the problem. Graphical results are presented and examined in detail.

2 Governing problems

Here, we consider the steady three-dimensional flow of an incompressible Maxwell fluid over a stretching surface at z=0. The flow takes place in the domain z>0. Heat and mass transfer characteristics are taken into account in the presence of internal heat generation/absorption and mixed convection. Convective heat and mass boundary conditions are considered. The ambient fluid temperature and concentration are taken as T_∞ and C_∞ while the surface temperature and concentration are maintained by convective heat and mass transfer at certain value T_f and C_f. The governing partial differential equations subject to boundary layer flow are

$$\frac{\partial u}{\partial x}+\frac{\partial v}{\partial y}+\frac{\partial w}{\partial z}=0 \tag{1}$$

$$u\frac{\partial u}{\partial x}+v\frac{\partial u}{\partial y}+w\frac{\partial u}{\partial z}=\nu\frac{\partial^2 u}{\partial z^2}-\lambda(u^2\frac{\partial^2 u}{\partial x^2}+v^2\frac{\partial^2 u}{\partial y^2}+w^2\frac{\partial^2 u}{\partial z^2}+2uv\frac{\partial^2 u}{\partial x\partial y}+2vw\frac{\partial^2 u}{\partial y\partial z}+2uw\frac{\partial^2 u}{\partial x\partial z})+g\left(\beta_\mathrm{T}(T-T_\infty)+\beta_\mathrm{C}(C-C_\infty)\right) \tag{2}$$

$$u\frac{\partial v}{\partial x}+v\frac{\partial v}{\partial y}+w\frac{\partial v}{\partial z}=\nu\frac{\partial^2 v}{\partial z^2}-\lambda(u^2\frac{\partial^2 v}{\partial x^2}+v^2\frac{\partial^2 v}{\partial y^2}+w^2\frac{\partial^2 v}{\partial z^2}+2uv\frac{\partial^2 v}{\partial x\partial y}+2vw\frac{\partial^2 v}{\partial y\partial z}+2uw\frac{\partial^2 v}{\partial x\partial z}) \tag{3}$$

$$\rho c_p(u\frac{\partial T}{\partial x}+v\frac{\partial T}{\partial y}+w\frac{\partial T}{\partial z})=k\frac{\partial^2 T}{\partial z^2}+Q(T-T_\infty) \tag{4}$$

$$u\frac{\partial C}{\partial x}+v\frac{\partial C}{\partial y}+w\frac{\partial C}{\partial z}=D\frac{\partial^2 C}{\partial z^2} \tag{5}$$

where the respective velocity components in the x-, y- and z-directions are denoted by u, v and w, λ is the relaxation time, ρ is the density of fluid, g is the gravitational acceleration, β_T and β_C are the thermal and concentration expansion coefficients, respectively, T is the fluid temperature, $\nu(=\mu/\rho)$ is the kinematic viscosity, μ is the dynamic viscosity of fluid, c_p is the specific heat, k is the thermal conductivity, Q is the uniform volumetric heat generation/absorption, C is the concentration field and D is the mass diffusivity.

The subjected boundary conditions are given by

$$u=u_\mathrm{e}=ax,\ v=by,w=0,\ -k\frac{\partial T}{\partial z}=h(T_\mathrm{f}-T),\ -D\frac{\partial C}{\partial z}=h^*(C_\mathrm{f}-C)\ \text{at}\ z=0 \tag{6}$$

$$u\to 0,v\to 0,T\to T_\infty,C\to C_\infty\ \text{as}\ z\to\infty \tag{7}$$

where h is the heat transfer coefficient, h^* is the concentration transfer coefficient, C_∞ is the ambient concentration, a and b are constants with unit s^{-1}.

We now define

$$\begin{cases} u = axf'(\eta) \\ v = ayg'(\eta) \\ w = -\sqrt{a\nu}(f(\eta)+g(\eta)) \\ \theta(\eta) = \dfrac{T-T_\infty}{T_\mathrm{f}-T_\infty} \\ \eta = z\sqrt{\dfrac{a}{\nu}} \\ \phi(\eta) = \dfrac{C-C_\infty}{C_\mathrm{w}-C_\infty} \end{cases} \tag{8}$$

The above variables satisfy Eq. (1) automatically while Eqs. (2)−(7) are converted to the following forms

$$f''' + (f+g)f'' - f'^2 + \beta_1[2(f+g)ff'' - (f+g)^2 f'''] + \lambda(\theta + N\phi) = 0 \tag{9}$$

$$g''' + (f+g)g'' - g'^2 + \beta_1[2(f+g)g'g'' - (f+g)^2 g'''] = 0 \tag{10}$$

$$\theta'' + Pr(f+g)\theta' + \beta_2\theta = 0 \tag{11}$$

$$\phi'' + Sc(f+g)\phi' = 0 \tag{12}$$

$$f = 0,\ g = 0,\ f' = 1,\ g' = \beta,\ \theta' = -\gamma_1(1-\theta(0)),\ \phi' = -\gamma_2(1-\phi(0))\ \text{ at } \eta = 0 \tag{13}$$

$$f' \to 0,\ g' \to 0,\ \theta \to 0,\ \phi \to 0\ \text{ as } \eta \to \infty \tag{14}$$

where β_1 is the dimensionless Deborah number, λ is the local buoyancy parameter, Gr_x is the local Grashof number, N is the concentration buoyancy parameter, Pr is the Prandtl number, β_2 is the heat generation absorption parameter, Sc is Schmidt number, β is the ratio of rates parameters, γ_1 and γ_2 are the Biot numbers and prime shows the differentiation with respect to η. These are given by

$$\begin{cases} \beta_1 = \lambda_1 a \\ \lambda = \dfrac{Gr_x}{Re_x^2} \\ Gr_x = \dfrac{g\beta_\mathrm{T}(T_\mathrm{f}-T_\infty)x^3}{\nu^2} \\ N = \dfrac{\beta_\mathrm{C}(C_\mathrm{w}-C_\infty)}{\beta_\mathrm{T}(T_\mathrm{f}-T_\infty)} \\ Pr = \dfrac{\nu}{\sigma} \\ \beta_2 = \dfrac{Q}{\rho c_p} \\ Sc = \dfrac{\nu}{D} \\ \beta = \dfrac{b}{a} \\ \gamma_1 = \dfrac{h}{k}\sqrt{\dfrac{\nu}{a}} \\ \gamma_2 = \dfrac{h^*}{D}\sqrt{\dfrac{\nu}{a}} \end{cases} \tag{15}$$

In dimensionless form, the local Nusselt and local Sherwood numbers are given by

$$\begin{cases} Nu/Re_x^{1/2} = -\theta'(0) \\ Sh/Re_x^{1/2} = -\phi'(0) \end{cases} \tag{16}$$

where $Re_x(=u_e x/\nu)$ is the local Reynolds number.

3 Series solutions

The initial approximations and auxiliary linear operators are required to develop homotopic solutions. We select the following initial guesses and linear operators for the present flow analysis:

$$\begin{cases} f_0(\eta) = \left(1-\mathrm{e}^{-\eta}\right) \\ g_0(\eta) = \beta\left(1-\mathrm{e}^{-\eta}\right) \\ \theta_0(\eta) = \dfrac{\gamma_1\exp(-\eta)}{1+\gamma_1} \\ \phi_0(\eta) = \dfrac{\gamma_2\exp(-\eta)}{1+\gamma_2} \end{cases} \tag{17}$$

$$\begin{cases} L_f = f''' - f' \\ L_g = g''' - g' \\ L_\theta = \theta'' - \theta \\ L_\phi = \phi'' - \phi \end{cases} \tag{18}$$

with the following properties of the defined operators in Eq. (18) i.e.

$$\begin{cases} L_f(C_1 + C_2\mathrm{e}^{\eta} + C_3\mathrm{e}^{-\eta}) = 0 \\ L_g(C_4 + C_5\mathrm{e}^{\eta} + C_6\mathrm{e}^{-\eta}) = 0 \\ L_\theta(C_7\mathrm{e}^{\eta} + C_8\mathrm{e}^{-\eta}) = 0 \\ L_\phi(C_9\mathrm{e}^{\eta} + C_{10}\mathrm{e}^{-\eta}) = 0 \end{cases} \tag{19}$$

where C_i (i=1−10) are the arbitrary constants.

The corresponding problems at the zeroth order deformations are given in the following forms:

$$(1-p)L_f\left[\hat{f}(\eta;p) - f_0(\eta)\right] = p\hbar_f \mathbf{N}_f\left[\hat{f}(\eta;p), \hat{g}(\eta;p), \hat{\theta}(\eta,p), \hat{\phi}(\eta,p)\right] \tag{20}$$

$$(1-p)L_g\left[\hat{g}(\eta;p) - g_0(\eta)\right] = p\hbar_g \mathbf{N}_g\left[\hat{f}(\eta;p), \hat{g}(\eta;p), \hat{\theta}(\eta,p), \hat{\phi}(\eta,p)\right] \tag{21}$$

$$(1-p)L_\theta\left[\hat{\theta}(\eta;p) - \theta_0(\eta)\right] = p\hbar_\theta \mathbf{N}_\theta\left[\hat{f}(\eta;p), \hat{g}(\eta;p), \hat{\theta}(\eta,p), \hat{\phi}(\eta,p)\right] \tag{22}$$

$$(1-p)L_\phi\left[\hat{\phi}(\eta;p) - \phi_0(\eta)\right] = p\hbar_\phi \mathbf{N}_\phi\left[\hat{f}(\eta;p), \hat{g}(\eta;p), \hat{\theta}(\eta,p), \hat{\phi}(\eta,p)\right] \tag{23}$$

$$\begin{cases}\hat{f}(0;p)=0\\ \hat{f}'(0;p)=1\\ \hat{f}'(\infty;p)=0\\ \hat{g}(0;p)=0\\ \hat{g}'(0;p)=\beta\\ \hat{g}'(\infty;p)=0\\ \hat{\theta}'(0,p)=-\gamma_1[1-\theta(0,p)]\\ \hat{\theta}(\infty,p)=0\\ \hat{\phi}'(0,p)=-\gamma_2[1-\hat{\phi}(0,p)]\\ \hat{\phi}(\infty,p)=0\end{cases} \tag{24}$$

$$\mathbf{N}_f[\hat{f}(\eta,p),\hat{g}(\eta,p),\hat{\theta}(\eta,p),\hat{\phi}(\eta,p)]=$$
$$\frac{\partial^3\hat{f}(\eta,p)}{\partial\eta^3}-\left(\frac{\partial\hat{f}(\eta,p)}{\partial\eta}\right)^2+(\hat{f}(\eta,p)+\hat{g}(\eta,p))$$
$$\frac{\partial^2\hat{f}(\eta,p)}{\partial\eta^2}+\beta_1\begin{bmatrix}2(\hat{f}(\eta,p)+\hat{g}(\eta,p))\\ \dfrac{\partial\hat{f}(\eta,p)}{\partial\eta}\dfrac{\partial^2\hat{f}(\eta,p)}{\partial\eta^2}\\ -(\hat{f}(\eta,p)+\hat{g}(\eta,p))^2\dfrac{\partial^3\hat{f}(\eta,p)}{\partial\eta^2}\end{bmatrix}+$$
$$\lambda[\hat{\theta}(\eta,p)+N_1\hat{\phi}(\eta,p)] \tag{25}$$

$$\mathbf{N}_g[\hat{g}(\eta,p),\hat{f}(\eta,p),\hat{\theta}(\eta,p),\hat{\phi}(\eta,p)]=$$
$$\frac{\partial^3\hat{g}(\eta,p)}{\partial\eta^3}-\left(\frac{\partial\hat{g}(\eta,p)}{\partial\eta}\right)^2+\hat{f}(\eta,p)+\hat{g}(\eta,p))$$
$$\frac{\partial^2\hat{g}(\eta,p)}{\partial\eta^2}+\beta_1\begin{bmatrix}2(\hat{f}(\eta,p)+\hat{g}(\eta,p))\\ \dfrac{\partial\hat{g}(\eta,p)}{\partial\eta}\dfrac{\partial^2\hat{g}(\eta,p)}{\partial\eta^2}\\ -(\hat{f}(\eta,p)+\hat{g}(\eta,p))^2\dfrac{\partial^3\hat{g}(\eta,p)}{\partial\eta^2}\end{bmatrix} \tag{26}$$

$$\mathbf{N}_\theta[\hat{\theta}(\eta,p),\hat{\phi}(\eta,p),\hat{f}(\eta,p),\hat{g}(\eta,p)]=$$
$$\frac{\partial^2\hat{\theta}(\eta,p)}{\partial\eta^2}+Pr(\hat{f}(\eta,p)+$$
$$\hat{g}(\eta,p))\frac{\partial\hat{\theta}(\eta,p)}{\partial\eta}+\beta_2\hat{\theta}(\eta,p) \tag{27}$$

$$\mathbf{N}_\phi[\hat{\phi}(\eta,p),\hat{\theta}(\eta,p),\hat{f}(\eta,p),\hat{g}(\eta,p)]=$$
$$\frac{\partial^2\hat{\phi}(\eta,p)}{\partial\eta^2}+Sc(\hat{f}(\eta,p)+\hat{g}(\eta,p))\frac{\partial\hat{\phi}(\eta,p)}{\partial\eta} \tag{28}$$

where p is an embedding parameter, the non-zero auxiliary parameters are $\hbar_f$, $\hbar_g$, $\hbar_\theta$ and $\hbar_\phi$ and the nonlinear operators are $\mathbf{N}_f$, $\mathbf{N}_g$, $\mathbf{N}_\theta$ and $\mathbf{N}_\phi$. When p=0 and p=1, one has

$$\begin{cases}\hat{f}(\eta;0)=f_0(\eta)\\ \hat{g}(\eta,0)=g_0(\eta)\\ \hat{\theta}(\eta,0)=\theta_0(\eta)\\ \hat{\phi}(\eta,0)=\phi_0(\eta)\\ \hat{f}(\eta;1)=f(\eta)\\ \hat{g}(\eta,1)=g(\eta)\\ \hat{\theta}(\eta,1)=\theta(\eta)\\ \hat{\phi}(\eta,1)=\phi_0(\eta)\end{cases} \tag{29}$$

Clearly, when p is increased from 0 to 1 then $f(\eta, p)$, $g(\eta, p)$, $\theta(\eta, p)$ and $\phi(\eta, p)$ vary from $f_0(\eta)$, $g_0(\eta)$, $\theta_0(\eta)$ and $\phi_0(\eta)$ to $f(\eta)$, $g(\eta)$, $\theta(\eta)$ and $\phi(\eta)$. By Taylor's expansion, we have

$$\begin{cases}f(\eta,p)=f_0(\eta)+\sum_{m=1}^{\infty}f_m(\eta)p^m\\ f_m(\eta)=\dfrac{1}{m!}\dfrac{\partial^m f(\eta;p)}{\partial p^m}\Big|_{p=0}\end{cases} \tag{30}$$

$$\begin{cases}g(\eta,p)=g_0(\eta)+\sum_{m=1}^{\infty}g_m(\eta)p^m\\ g_m(\eta)=\dfrac{1}{m!}\dfrac{\partial^m g(\eta;p)}{\partial p^m}\Big|_{p=0}\end{cases} \tag{31}$$

$$\begin{cases}\theta(\eta,p)=\theta_0(\eta)\sum_{m=1}^{\infty}\theta_m(\eta)p^m\\ \theta_m(\eta)=\dfrac{1}{m!}\dfrac{\partial^m\theta(\eta;p)}{\partial p^m}\Big|_{p=0}\end{cases} \tag{32}$$

$$\begin{cases}\phi(\eta,p)=\phi_0(\eta)\sum_{m=1}^{\infty}\phi_m(\eta)p^m\\ \phi_m(\eta)=\dfrac{1}{m!}\dfrac{\partial^m\phi(\eta;p)}{\partial p^m}\Big|_{p=0}\end{cases} \tag{33}$$

where the convergence of the above series strongly depends upon $\hbar_f$, $\hbar_g$, $\hbar_\theta$ and $\hbar_\phi$. Considering that $\hbar_f$, $\hbar_g$, $\hbar_\theta$ and $\hbar_\phi$ are selected properly, Eqs. (30)−(33) converge at p=1, and then we have

$$f(\eta)=f_0(\eta)+\sum_{m=1}^{\infty}f_m(\eta) \tag{34}$$

$$g(\eta)=g_0(\eta)+\sum_{m=1}^{\infty}g_m(\eta) \tag{35}$$

$$\theta(\eta)=\theta_0(\eta)+\sum_{m=1}^{\infty}\theta_m(\eta) \tag{36}$$

$$\phi(\eta)=\phi_0(\eta)+\sum_{m=1}^{\infty}\phi_m(\eta) \tag{37}$$

The general solutions can be expressed below:

$$f_m(\eta)=f_m^*(\eta)+C_1+C_2\mathrm{e}^{\eta}+C_3\mathrm{e}^{-\eta} \tag{38}$$

$$g_m(\eta)=g_m^*(\eta)+C_4+C_5\mathrm{e}^{\eta}+C_6\mathrm{e}^{-\eta} \quad (39)$$

$$\theta_m(\eta)=\theta_m^*(\eta)+C_7\mathrm{e}^{\eta}+C_8\mathrm{e}^{-\eta} \quad (40)$$

$$\phi_m(\eta)=\phi_m^*(\eta)+C_9\mathrm{e}^{\eta}+C_{10}\mathrm{e}^{-\eta} \quad (41)$$

where f_m^*, g_m^*, θ_m^* and ϕ_m^* indicate the special solutions.

4 Convergence analysis and discussion

Clearly, the homotopic series solutions (34)−(37) depend on the auxiliary parameters $\hbar_f$, $\hbar_g$, $\hbar_\theta$ and $\hbar_\phi$. These parameters have important role in the convergence of series solutions. For this purpose, the $\hbar$-curves are drawn at 15th order of approximations to determine the suitable ranges of these auxiliary parameters. Figure 1 shows that the acceptable values of $\hbar_f$, $\hbar_g$, $\hbar_\theta$ and $\hbar_\phi$ are $-1.4\le\hbar_f\le-0.20$, $-1.6\le\hbar_g\le-0.40$ and $-1.50\le\hbar_\theta$, $\hbar_\phi\le-0.30$. Table 1 ensures the convergence of homotopic series solutions in the whole region of η when $\hbar_f=\hbar_g=\hbar_\theta=\hbar_\phi=-0.5$.

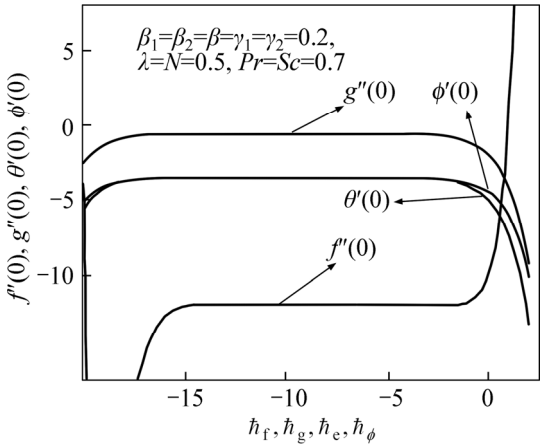

Fig. 1 $\hbar$-curves for functions $f(\eta)$, $g(\eta)$, $\theta(\eta)$ and $\varphi(\eta)$

Table 1 Convergence of series solutions for different order of approximations when $\beta=\beta_1=\beta_2=0.2$, $\gamma_2=\lambda=N=0.3$, $\gamma_1=0.5$, $Sc=1.0$, $Pr=1.2$ and $\hbar_f=\hbar_g=\hbar_\theta=\hbar_\phi=-0.5$

Order of approximation	$-f''(0)$	$-g''(0)$	$-\theta'(0)$	$-\phi'(0)$
1	1.018	0.1497	0.3133	0.2228
5	1.029	0.06217	0.2782	0.2095
10	1.028	0.03940	0.2703	0.2067
15	1.029	0.03866	0.2702	0.2066
20	1.029	0.03982	0.2705	0.2066
25	1.029	0.03993	0.2705	0.2066
30	1.029	0.03993	0.2705	0.2066

Figures 2−11 show the effects of Deborah number β_1, stretching ratio parameter β, mixed convection parameter λ, concentration buoyancy parameter N and internal heat generation/absorption parameter β_2 on the velocity profiles $f'(\eta)$ and $g'(\eta)$. Figures 2 and 3 are drawn to see the behavior of Deborah number β_1 on the velocity profiles $f'(\eta)$ and $g'(\eta)$. It is found that both the velocity profiles $f'(\eta)$ and $g'(\eta)$ decrease with an enhancement in β_1. It is also examined from these figures that associated boundary layer thicknesses are decreasing functions of β_1. This is due to the fact that β_1 depends on relaxation time. Larger relaxation time offers more resistance to the flow due to which the velocities are decreased. Effects of stretching ratio parameter β on the velocity profiles $f'(\eta)$ and $g'(\eta)$ are depicted in Figs. 4 and 5. Opposite behavior for the velocity profiles $f'(\eta)$ and $g'(\eta)$ are examined with an increase in stretching ratio parameter β. Figures 6 and 7 are displayed to see the impact of mixed convection parameter λ on the velocity profiles $f'(\eta)$ and $g'(\eta)$. It is seen that both the velocity profiles $f'(\eta)$ and $g'(\eta)$ increase with an enhancement in λ. Also, momentum boundary layer thicknesses are increased with an increase in λ. In fact, an increase in λ enhances the buoyancy forces which are more dominant to viscous forces. Variations of concentration buoyancy parameter N on the velocity profiles $f'(\eta)$ and $g'(\eta)$ are displayed in Figs. 8 and 9. Similar behavior of N is noted on the velocity profiles $f'(\eta)$ and $g'(\eta)$. Figures 10 and 11 elucidate the influence of internal heat generation/ absorption parameter on the velocity profiles $f'(\eta)$ and $g'(\eta)$. For the case of heat

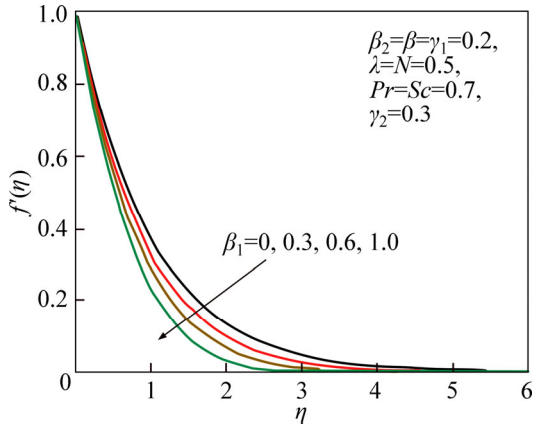

Fig. 2 Influence of β_1 on $f'(\eta)$

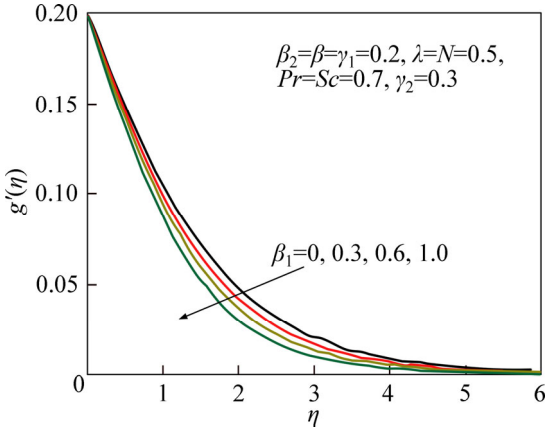

Fig. 3 Influence of β_1 on $g'(\eta)$

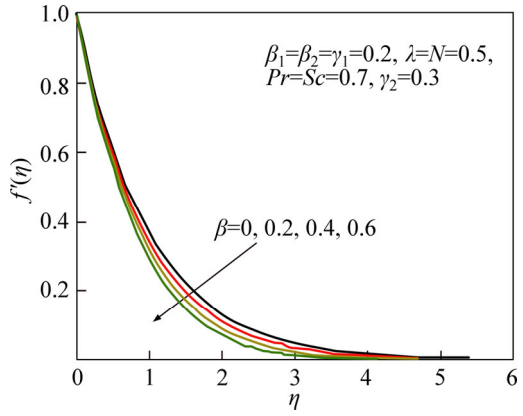

Fig. 4 Influence of β on $f'(\eta)$

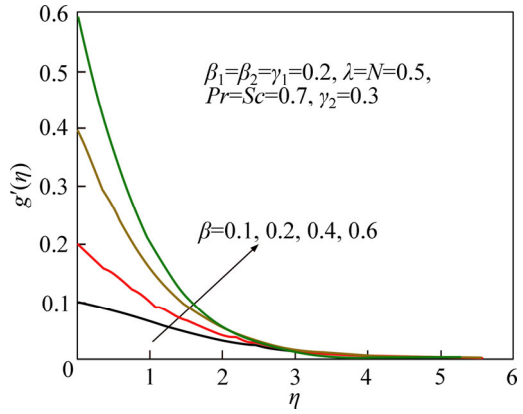

Fig. 5 Influence of β on $g'(\eta)$

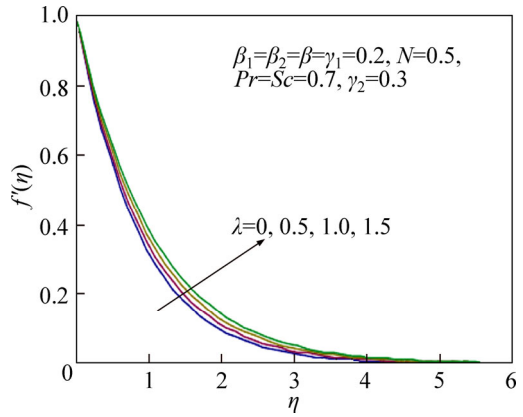

Fig. 6 Influence of λ on $f'(\eta)$

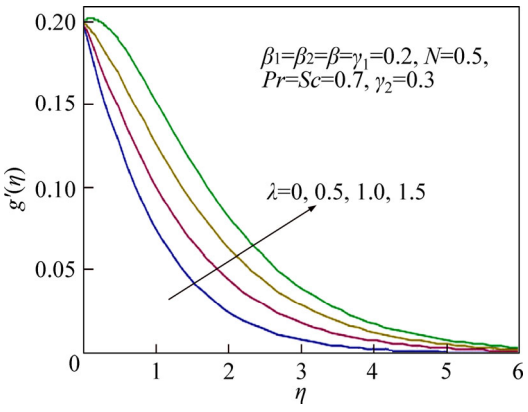

Fig. 7 Influence of λ on $g'(\eta)$

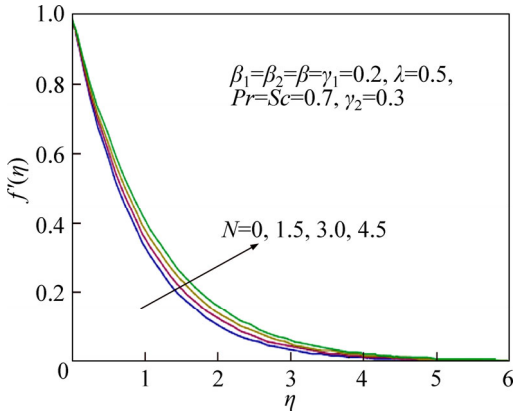

Fig. 8 Influence of N on $f'(\eta)$

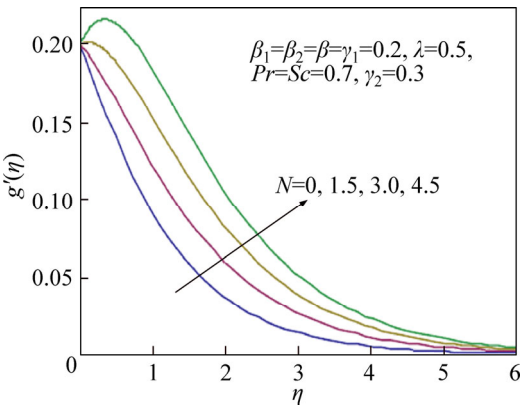

Fig. 9 Influence of N on $g'(\eta)$

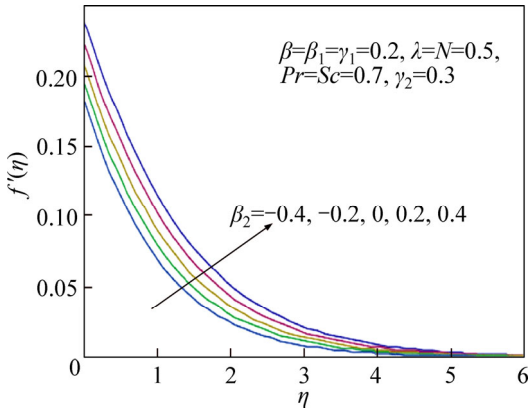

Fig. 10 Influence of β_2 on $f'(\eta)$

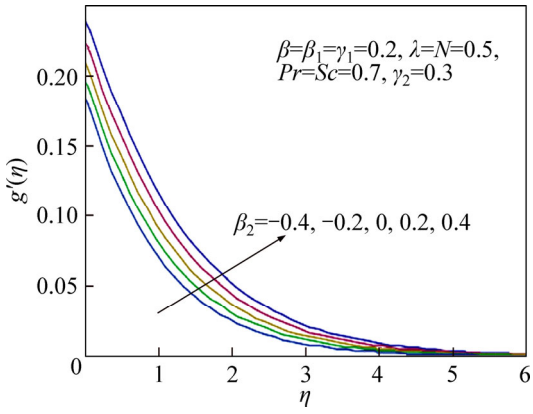

Fig. 11 Influence of β_2 on $g'(\eta)$

generation $\beta_2>0$, both the velocity profiles $f'(\eta)$ and $g'(\eta)$ increase. Also the associated momentum boundary layer thicknesses increase with the heat generation $\beta_2>0$, while in the case of heat absorption $\beta_2<0$, the opposite behavior is seen.

Figures 12−15 are plotted to see the variations of internal heat generation/absorption parameter β_2, stretching ratio parameter β, heat transfer Biot number γ_1 and Prandtl number Pr on the temperature $\theta(\eta)$. It is found from Fig. 12 that the thermal boundary layer thickness and temperature $\theta(\eta)$ are increasing functions of internal heat generation parameter $\beta_2>0$ and decreasing functions of internal heat absorption $\beta_2<0$. Effect of stretching ratio parameter β on temperature $\theta(\eta)$ is analyzed in Fig. 13. It is noticed that both thermal boundary layer thickness and temperature $\theta(\eta)$ decrease when larger values of β are used. With an increase in heat transfer Biot number γ_1, both the thermal boundary layer thickness and temperature $\theta(\eta)$ are enhanced (see Fig. 14). The reason is that γ_1 depends on heat transfer coefficient h which leads to an increase in temperature $\theta(\eta)$. Effect of Prandtl number Pr shows a reduction in the temperature and thermal boundary layer thickness (see Fig. 15). This is due to the fact that Prandtl number Pr is the ratio of momentum to thermal diffusivity. When Pr increases, thermal diffusivity reduces, as a result, temperature and thermal boundary layer thickness are decreased.

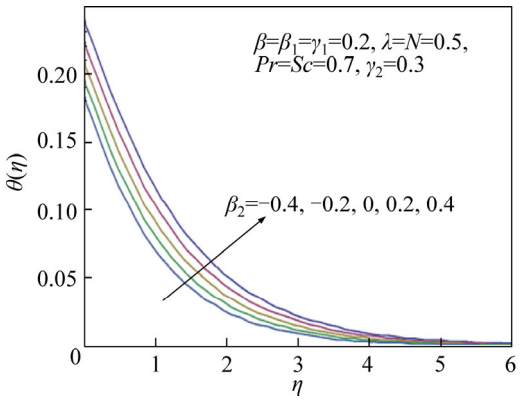

Fig. 12 Influence of β_1 on $\theta(\eta)$

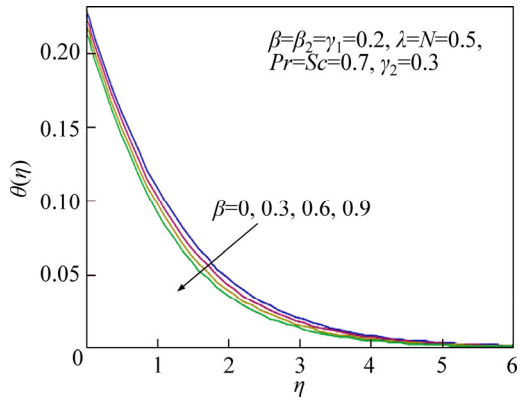

Fig. 13 Influence of β on $\theta(\eta)$

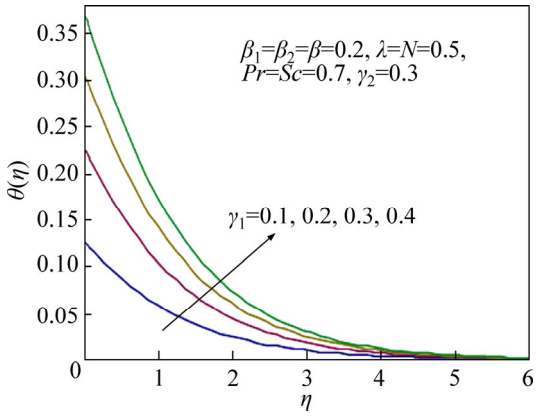

Fig. 14 Influence of γ_1 on $\theta(\eta)$

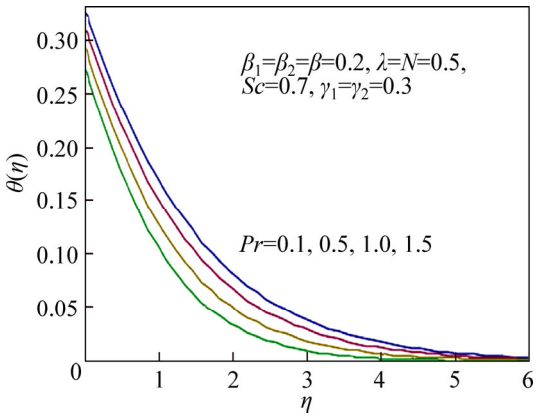

Fig. 15 Influence of Pr on $\theta(\eta)$

Figures 16−18 are displayed to analyze the behavior of concentration $\phi(\eta)$ for different values of stretching ratio parameter β, mass transfer Biot number γ_2 and Schmidt number Sc. Figure 16 is drawn to analyze the effect of stretching ratio parameter β on the concentration profile $\phi(\eta)$. It is found that the fluid concentration $\phi(\eta)$ and boundary layer thickness decrease with an increase in stretching ratio parameter β. Effect of mass transfer Biot number γ_2 on the concentration profile $\phi(\eta)$ is elucidated in Fig. 17. It is observed that as γ_2 increases, the associated boundary layer thickness and concentration profile $\phi(\eta)$ grow. As mass transfer Biot

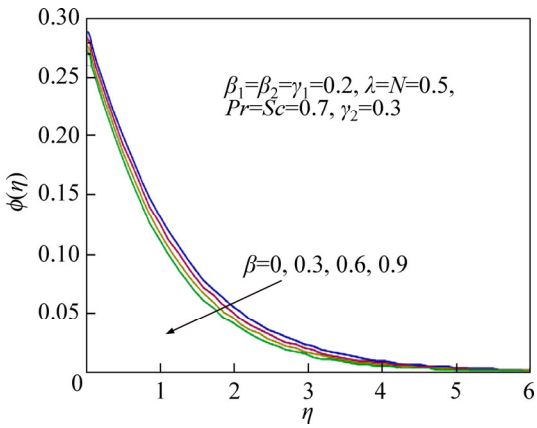

Fig. 16 Influence of β on $\phi(\eta)$

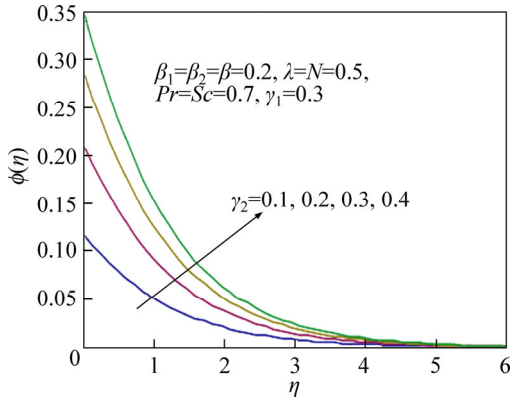

Fig. 17 Influence of γ_2 on $\phi(\eta)$

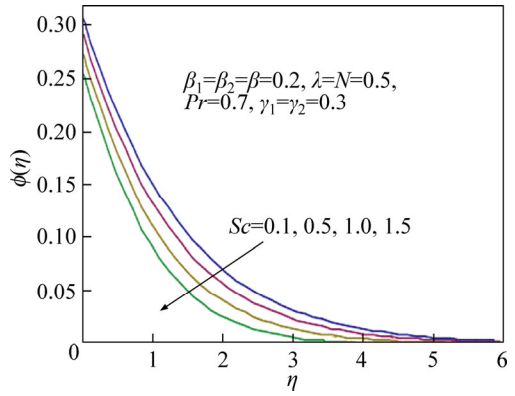

Fig. 18 Influence of Sc on $\phi(\eta)$

number γ_2 depends on mass transfer coefficient h^*, with an enhancement in γ_2, the mass transfer coefficient increases, which leads to an increase in concentration profile $\phi(\eta)$. Behavior of Schmidt number Sc on the fluid concentration $\phi(\eta)$ is presented in Fig. 18. As Sc is the relation of momentum to mass diffusivities, with an increase in Sc, the mass diffusivity decreases, due to which the concentration $\phi(\eta)$ decreases (see Fig. 18).

Impacts of mixed convection parameter λ, concentration buoyancy parameter N, Deborah number β_1, internal heat generation/absorption parameter β_2, heat transfer Biot number γ_1 and Prandtl number Pr on the local Nusselt number ($-\theta'(0)$) are displayed in Figs. 19−21. It is found that local Nusselt number ($-\theta'(0)$) enhances with an increase in λ and N (see Fig. 19). Local Nusselt number ($-\theta'(0)$) reduces with internal heat generation parameter $\beta_2>0$ while it increases with internal heat absorption parameter $\beta_2<0$ (see Fig. 20). It is also noticed from Fig. 20 that local Nusselt number ($-\theta'(0)$) decreases with an increase in β_1. Figure 21 depicts that the local Nusselt number ($-\theta'(0)$) is an increasing function of heat transfer Biot number γ_1 and Prandtl number Pr.

Figures 22−24 are sketched to see the variations of mixed convection parameter λ, concentration buoyancy parameter N, Deborah number β_1, internal heat generation/absorption parameter β_2, mass transfer Biot

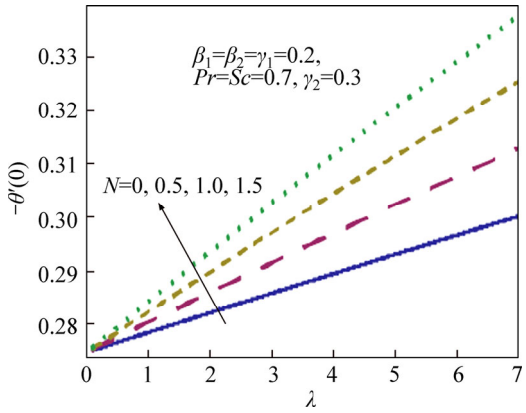

Fig. 19 Influences of λ and N on $-\theta'(0)$

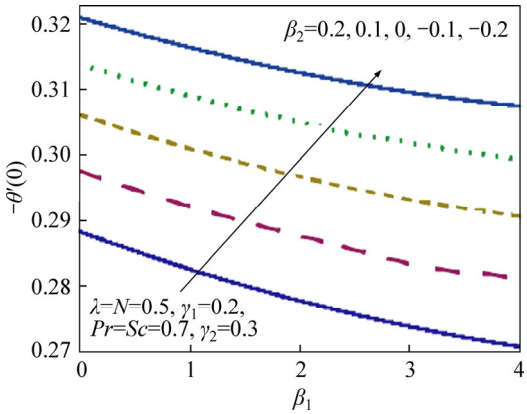

Fig. 20 Influences of β_1 and β_2 on $-\theta'(0)$

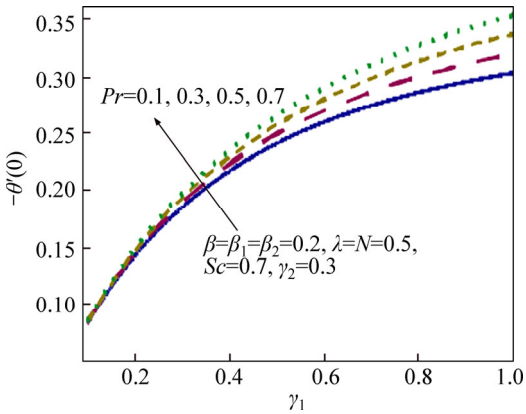

Fig. 21 Influences of γ_1 and Pr on $-\theta'(0)$

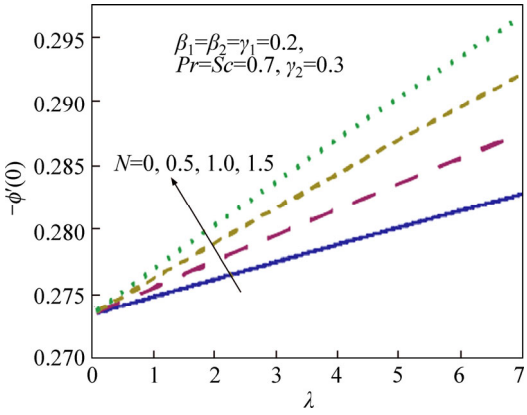

Fig. 22 Influences of λ and N on $-\phi'(0)$

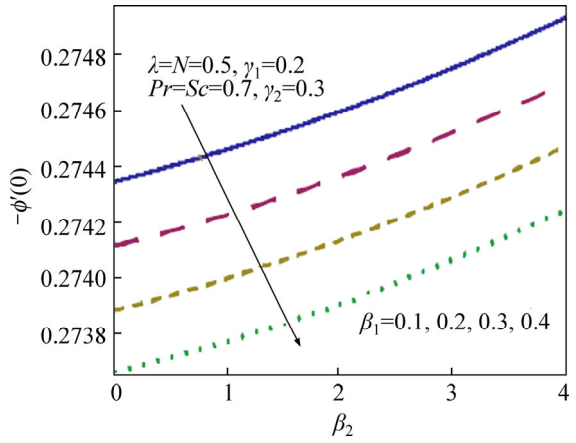

Fig. 23 influences of β_1 and β_2 on $-\phi'(0)$

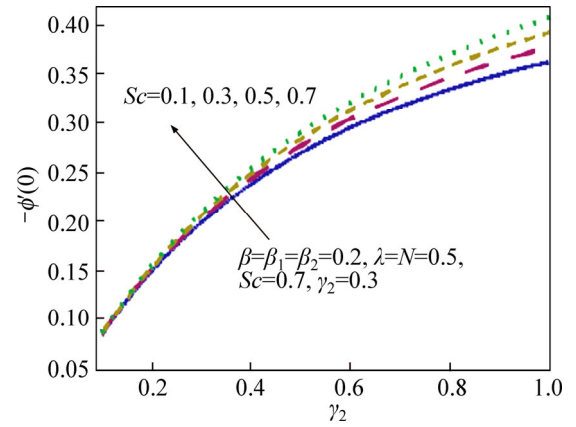

Fig. 24 Influences of γ_2 and Sc on $-\varphi'(0)$

number γ_2 and Schmidt number Sc on the Sherwood number $(-\phi'(0))$. Figure 22 shows that the Sherwood number $(-\phi'(0))$ increases with an increase in λ and N. Figure 23 indicates that the Sherwood number $(-\phi'(0))$ increases by increasing internal heat generation $\beta_2>0$ while reverse effect is examined with an increase in Deborah number β_1. Sherwood number $(-\phi'(0))$ is an increasing function of both mass transfer Biot number γ_2 and Schmidt number Sc (see Fig. 24).

5 Conclusions

1) Three-dimensional mixed convection flow of Maxwell fluid over a stretching sheet with internal heat generation/absorption is analyzed. Convective boundary conditions for both heat and mass are considered.

2) Both thermal and concentration boundary layer thicknesses are decreasing functions of stretching ratio parameter β. Variations of mixed convection parameter λ and concentration buoyancy parameter N on the velocity profiles and associated boundary layer thicknesses are enhanced. Velocity profiles and temperature increase in the case of internal heat generation $\beta_2>0$ while they reduce for heat absorption $\beta_2<0$. Heat transfer Biot number γ_1 increases the thermal boundary layer thickness and temperature. Also, concentration and its associated boundary layer are enhanced with an increase in mass transfer Biot number γ_2.

3) The local Nusselt and Sherwood numbers have quite similar behaviors for increasing values of mixed convection parameter λ, concentration buoyancy parameter N and Deborah number β_1. Larger values of Prandtl number Pr, heat absorption parameter $\beta_2<0$ and heat transfer Biot number γ_1 give rise to the local Nusselt number $(-\theta'(0))$. Sherwood number $(-\phi'(0))$ enhances with an increase in heat generation $\beta_2>0$, Schmidt number Sc and mass transfer Biot number γ_2.

References

[1] CRANE L J. Flow past a stretching plate [J]. Z Angew Math Physk, 1970, 21: 645−647.

[2] JALIL M, ASGHAR S. Flow of power-law fluid over a stretching surface: A Lie group analysis [J]. International Journal of Non-Linear Mechanics, 2013, 48: 65−71.

[3] AHMAD A, ASGHAR S. Flow of a second grade fluid over a sheet stretching with arbitrary velocities subject to a transverse magnetic field [J]. Applied Mathematics Letters, 2011, 24: 1905−1909.

[4] HAYAT T, SHEHZAD S A, QASIM M, OBAIDAT S. Flow of a second grade fluid with convective boundary conditions [J]. Thermal Science, 2011, 15: 253−S261.

[5] JAMIL M, RAUF A, FETECAU C, KHAN N A. Helical flows of second grade fluid due to constantly accelerated shear stresses [J]. Communications in Nonlinear Science and Numerical Simulation, 2011, 16: 1959−1969.

[6] HAYAT T, NAZ R, ALSAEDI A, RASHIDI M M. Hydromagnetic rotating flow of third grade fluid [J]. Applied Mathematics and Mechanics, 2013, 34: 1481−1494.

[7] ABBASBANDY S, HAYAT T. On series solution for unsteady boundary layer equations in a special third grade fluid [J]. Communications in Nonlinear Science and Numerical Simulation, 2011, 16: 3140−3146.

[8] SHEHZAD S, QASIM M, HAYAT T, SAJID M, OBAIDAT S, Boundary layer flow of Maxwell fluid with power law heat flux and heat source [J]. International Journal of Numerical Methods for Heat & Fluid Flow, 2013, 23: 1225−1241.

[9] MUKHOPADHYAY S. Heat transfer analysis of the unsteady flow of a Maxwell Fluid over a stretching surface in the presence of a heat source/sink [J]. Chinese Physics Letters, 2012, 29:054703.

[10] ABBAS Z, WANG Y, HAYAT T, OBERLACK M. Mixed convection in the stagnation-point flow of a Maxwell fluid towards a vertical stretching surface [J]. Nonlinear Analysis: Real World Applications, 2010, 121; 3218−3228.

[11] MUKHOPADHYAY S. Effects of slip on unsteady mixed convective flow and heat transfer past a stretching surface [J]. Chinese Physics Letters, 2010, 27: 124401.

[12] RASHIDI M M, ASHRAF M, ROSTAMI B, RASTEGARI M T, BASHIR S. Mixed convection boundary layer flow of a Micropolar fluid towards a heated shrinking sheet by homotopy analysis method [J]. Thermal Science, 2013, doi:10.2298/TSCI130212096R.

[13] MORADI A, AHMADIKIA H, HAYAT T, ALSAEDI A. On mixed convection-radiation interaction about an inclined plate through a porous medium [J]. International Journal of Thermal Sciences, 2013, 64: 129−136.

[14] TURKYILMAZOGLU M. The analytical solution of mixed

convection heat transfer and fluid flow of a MHD viscoelastic fluid over a permeable stretching surface [J]. International Journal of Mechanical Sciences, 2013, 77: 263−268.

[15] ELBASHBESHY E M A, ALDAWODY D A. Heat transfer over an unsteady stretching surface with variable heat flux in the presence of a heat source or sink [J]. Computers & Mathematics with Applications, 2010, 60: 2806−2811.

[16] HAYAT T, SHEHZAD S A, QASIM M, OBAIDAT S. Radiative flow of Jeffery fluid in a porous medium with power law heat flux and heat source [J]. Nuclear Engineering and Design, 2012, 243: 15−19.

[17] KANDASAMY R, HAYAT T, OBAIDAT S. Group theory transformation for Soret and Dufour effects on free convective heat and mass transfer with thermophoresis and chemical reaction over a porous stretching surface in the presence of heat source/sink [J]. Nuclear Engineering and Design, 2011, 241: 2155−2161.

[18] AZIZ A. A similarity solution for laminar thermal boundary layer over a flat plate with a convective surface boundary condition [J]. Communications in Nonlinear Science and Numerical Simulation, 2009, 14: 1064−1068.

[19] MAKINDE O D, AZIZ A. Boundary layer flow of a nanofluid past a stretching sheet with a convective boundary condition [J]. International Journal of Thermal Sciences, 2011, 50: 1326−1332.

[20] SHEHZAD S A, HAYAT T, ALSAEDI A. Three-dimensional flow of Jeffery fluid with convective surface boundary conditions [J]. International Journal of Heat and Mass Transfer, 2012, 55: 3971−3976.

[21] LIAO S J. Homotopy analysis method in nonlinear differential equations [M]. Beijing: Higher Education Press, Beijing and Springer-Verlag Berlin Heidelberg, 2012: 15−26.

[22] ABBASBANDY S, HASHEMI M S, HASHIM I. On convergence of homotopy analysis method and its application to fractional integro-differential equations [J]. Quaestiones Mathematicae, 2013, 36: 93−105.

[23] ZHENG L, NIU J, ZHANG X, GAO Y. MHD flow and heat transfer over a porous shrinking surface with velocity slip and temperature jump [J]. Mathematical and Computer Modelling, 2012, 56: 133−144.

[24] RASHIDI M M, RAJVANSHI S C, KEIMANESH M. Study of Pulsatile flow in a porous annulus with the homotopy analysis method [J]. International Journal of Numerical Method For Heat & Fluid Flow, 2012, 22: 971−989.

[25] HASSAN H N, RASHIDI M M. An analytic solution of micropolar flow in a porous channel with mass injection using homotopy analysis method [J]. International Journal of Numerical Method For Heat & Fluid Flow, 2014, 2: 419−437.

[26] TURKYILMAZOGLU M. Solution of Thomas-Fermi equation with a convergent approach [J]. Communications in Nonlinear Science and Numerical Simulation, 2012, 17: 4097−4103.

[27] HAYAT T, SHEHZAD S A, ASHRAF M B, ALSAEDI A. Magnetohydrodynamic mixed convection flow of thixotropic fluid with thermophoresis and Joule heating [J]. Journal of Thermophysics and Heat Transfer, 2013, 27: 733−740.

[28] RAMZAN M, FAROOQ M, ALSAEDI A, HAYAT T. MHD three-dimensional flow of couple stress fluid with Newtonian heating [J]. European Physical Journal Plus, 2013, 128: 49.

[29] ALSAADI F E, SHEHZAD S A, HAYAT T, MONAQUEL S J. Soret and Dufour effects on the unsteady mixed convection flow over a stretching surface [J]. Journal of Mechanics, 2013, 29: 623−632.

[30] HAYAT T, ASHRAF M B, ALSULAMI HH, ALHUTHALI M S. Three-dimensional mixed convection flow of viscoelastic fluid with thermal radiation and convective conditions [J]. Plos One, 2014, 9: e90038.

(Edited by FANG Jing-hua)